Mon. Not. R. Astron. Soc. **348,** 987–998 (2004) doi:10.1111/j.1365-2966.2004.07426.x

Colour variability of asteroids in the Sloan Digital Sky Survey Moving Object Catalog

Gy. M. Szabó,[1,2]★ Ž. Ivezić,[3]† M. Jurić,[3] R. Lupton[3] and L. L. Kiss[1,4]

[1]*Department of Experimental Physics and Astronomical Observatory, University of Szeged, 6720 Szeged, Hungary*
[2]*Department of Physics and Astronomy, Johns Hopkins University, Baltimore, MD 21218, USA*
[3]*Princeton University Observatory, Princeton, NJ 08544, USA*
[4]*University of Sydney, School of Physics, Sydney, Australia*

Accepted 2003 November 12. Received 2003 November 12; in original form 2003 August 29

ABSTRACT

We report a detection of statistically significant colour variations for a sample of 7531 multiply observed asteroids that are listed in the Sloan Digital Sky Survey Moving Object Catalog. Using five-band photometric observations accurate to ∼0.02 mag, we detect colour variations in the range 0.06–0.11 mag (rms). These variations appear to be uncorrelated with the physical characteristics of the asteroids, such as diameter (in the probed 1–10 km range), taxonomic class and family membership. Despite this lack of correlation, which implies a random nature for the cause of colour variability, a suite of tests suggest that the detected variations are not instrumental effects. In particular, the observed colour variations are incompatible with photometric errors, and, for objects observed at least four times, the colour change in the first pair of observations is correlated with the colour change in the second pair. These facts strongly suggest that the observed effect is real, and also indicate that colour variations are larger for some asteroids than for others. The detected colour variations can be explained as being due to inhomogeneous albedo distribution over an asteroid's surface. Although relatively small, these variations suggest that fairly large patches with different colour than their surroundings exist on a significant fraction of asteroids. This conclusion is in agreement with spatially resolved colour images of several large asteroids obtained by the *Near Earth Asteroid Rendezvous* (*NEAR*) spacecraft and the *Hubble Space Telescope* (*HST*).

Key words: minor planets, asteroids – Solar system: general.

1 INTRODUCTION

Asteroids are rotating aspherical reflective bodies which thus exhibit brightness variations. As recognized long ago (Russell 1906; Metcalf 1907), studies of their light curves provide important constraints on their physical properties and processes that affect their evolution. For example, well-sampled and accurate light curves can be used to determine asteroid asphericity, spin vector and even albedo inhomogeneity across the surface (Magnusson 1991). Current knowledge about asteroid rotation rates and light-curve properties is well summarized by Pravec & Harris (2000). The rotational periods range from ∼2 h to ∼15 h. The light-curve amplitudes for main-belt asteroids and near-Earth objects are typically of the order 0.1–0.2 mag (peak-to-peak). Recently, similar variations have been detected for a dozen Kuiper Belt objects (Sheppard & Jewitt 2002). The largest amplitudes of ∼2 mag (peak-to-peak) are observed for asteroids 1865 Cerberus and 1620 Geographos (Wisniewski et al. 1997; Szabó et al. 2001).

In contrast to appreciable and easily detectable amplitudes of single-band light curves, typical asteroid colour variations are much smaller. Indeed, if albedo did not vary across an asteroid's surface, then the asteroid would not display colour variability irrespective of its geometry.[1] While the absence of colour variability may also be consistent with a grey albedo variation, the strong observed correlation between asteroid albedo and colour [blue C-type asteroids have visual albedo of $p_V \sim 0.04$, while for red S-type asteroids $p_V \sim 0.15$–0.20 (Zellner 1979; Shoemaker et al. 1979)] implies that non-uniform albedo distribution should be detectable through colour variability. Following Magnusson (1991), we shall refer to non-uniform albedo distribution across an asteroid surface as albedo variegation.

The most notable case of albedo variegation is displayed by 4 Vesta, which apparently has one bright and one dark hemisphere

★E-mail: szgy@mcse.hu, szgy@astro.u-szeged.hu
†H. N. Russell Fellow.

[1] Apart from the so-called differential albedo effect (Bowell & Lumme 1979).

(Blanco & Catalano 1979; Degewij, Tedesco & Zellner 1979; Binzel et al. 1997). Definite colour variations have been detected in only a few dozen asteroids. A colour variability at the level of a few per cent has been measured directly for Eros ($V-R$ and $V-I$, Wisniewski 1976) and for 51 Nemausa ($u-b$ and $v-y$, Gammelgaard & Kristensen 1991). In a study that still remains one of the largest monitoring programmes for colour variability, Degewij et al. (1979) detected colour variations greater than 0.03 mag in six out of 24 monitored asteroids. In another notable study, Schober & Schroll (1982) detected colour modulation in 49 asteroids. Recently, a spectacular confirmation of albedo variegation has been obtained for Eros by *NEAR* multispectral imaging (Murchie et al. 2002). While similar spatially resolved images are available for several other objects (e.g. Zellner et al. 1997; Binzel et al. 1997; Baliunas et al. 2003), the number of asteroids with observational constraints on their albedo variegation remains small.

Here we study asteroid colour variability by utilizing the Sloan Digital Sky Survey Moving Object Catalog (SDSSMOC, Ivezić et al. 2002a). SDSSMOC currently contains accurate (0.02 mag) five-band photometric measurements for over 130 000 asteroids. A fraction of these objects are previously recognized asteroids with available orbits, and 7531 of them were observed by SDSS at least twice. We use the colour differences between the two observations of the same objects to constrain the ensemble properties, as opposed to studying well-sampled light curves for a small number of objects. The lack of detailed information for individual objects is substituted by the large sample size, which allows us to study correlations between colour variability and various physical properties in a statistical sense. Also, objects in the sample studied here have typical sizes 1–10 km, about a factor of 10 smaller than objects for which colour variations have been reported in the literature.

We describe the SDSSMOC and data selection in Section 2, and in Section 3 we perform various tests to demonstrate that detected colour variability of multiply observed objects is not an observational artefact. In Section 4 we search for correlations between the colour variability and asteroid physical properties, and summarize our results in Section 5.

2 SDSS OBSERVATIONS OF MOVING OBJECTS

SDSS is a digital photometric and spectroscopic survey which will cover 10 000 deg^2 of the celestial sphere in the North Galactic Cap and a smaller ($\sim$225 deg^2) and deeper survey in the Southern Galactic hemisphere (Azabajian et al. 2003, and references therein). The survey sky coverage will result in photometric measurements for about 50 million stars and a similar number of galaxies. About 50 per cent of the survey is currently finished. The flux densities of detected objects are measured almost simultaneously in five bands (u, g, r, i and z, Fukugita et al. 1996) with effective wavelengths of 3551, 4686, 6166, 7480 and 8932 Å, 95 per cent complete for point sources to limiting magnitudes of 22.0, 22.2, 22.2, 21.3 and 20.5 in the North Galactic Cap. Astrometric positions are accurate to about 0.1 arcsec per coordinate (rms) for sources brighter than 20.5 mag, and the morphological information from the images allows robust star–galaxy separation (Lupton et al. 2001) to $\sim$21.5 mag.

SDSS, although primarily designed for observations of extragalactic objects, is contributing significantly to studies of Solar system objects, because asteroids in the imaging survey must be explicitly detected to avoid contamination of the samples of extragalactic objects selected for spectroscopy. Preliminary analysis of SDSS commissioning data (Ivezić et al. 2001, hereafter I01) showed that SDSS will increase the number of asteroids with accurate five-colour photometry by more than two orders of magnitude, and to a limit about five magnitudes fainter (seven magnitudes when the completeness limits are compared) than previous multicolour surveys (e.g. The Eight Color Asteroid Survey, Zellner, Tholen & Tedesco 1985).

2.1 Sample selection using the SDSS Moving Object Catalog

The SDSS Moving Object Catalog[2] is a public, value-added catalogue of SDSS asteroid observations. In addition to providing SDSS astrometric and photometric measurements, all observations are matched to known objects listed in the AST–ORB file (Bowell 2001), and to the data base of proper orbital elements (Milani 1999), as described in detail by (Jurić et al. 2002, hereafter J02). Multiple SDSS observations of objects with known orbital parameters can be accurately linked, and thus SDSSMOC contains rich information about asteroid colour variability.

We select 7531 multiply observed objects from the second SDSSMOC edition (ADR2.dat) by requiring that the number of observations ($N_{\rm ap}$) is at least two, and use the first and second observations to compute photometric changes. A 'high-quality' sample of 2289 asteroids is defined by two additional restrictions:

(i) In order to avoid the increased photometric errors at the faint end, we require $r < 19$.

(ii) In order to minimize the effect of variable angle from the opposition on the observed colour, we select only objects for which the change of this angle is less than 1.5°.

We also utilize a subsample of 541 asteroids that were observed at least four times.

Since SDSS observations of asteroids are essentially random, and the time between them (days to months – 75 per cent of repeated observations are obtained within three months, and 86 per cent within a year) is much longer than typical rotational periods (<1 d), the phases of any two repeated observations are practically uncorrelated. Thus, the distribution of magnitude and colour changes for a large ensemble of asteroids is a good proxy for random two-epoch sampling of an asteroid's single-band and colour light curves. Of course, this is strictly true only if the distributions of amplitudes and shapes of these light curves are fairly narrow. For wide distributions of amplitudes and shapes, the observed two-epoch magnitude and colour changes represent convolution of the two effects.

3 ASTEROID COLOUR VARIABILITY IN SDSSMOC

The colours of asteroids in the SDSS photometric system are discussed in detail by I01. They defined a principal colour in the $r-i$ versus $g-r$ colour–colour diagram, a, as

$$a \equiv 0.89(g-r) + 0.45(r-i) - 0.57. \quad (1)$$

The a colour distribution is strongly bimodal (see fig. 9 in I01), with the two modes at -0.1 and 0.1. The rms scatter around each mode is about 0.05 mag. The two modes are associated with different taxonomic classes: the 'blue' mode includes C, E, M and P types; and the 'red' mode includes S, D, A, V and J types (see fig. 10 in I01). The Vesta-type asteroids (type V) can be effectively separated

[2] Available at http://www.sdss.org

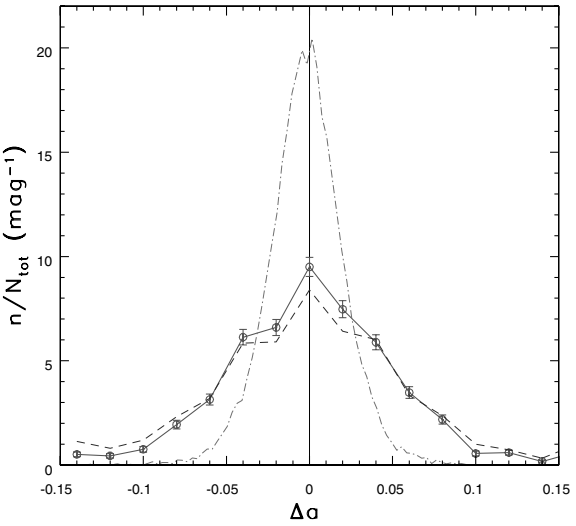

Figure 1. The dashed line shows the distribution of the *a* colour change between two epochs for all 7531 asteroids from SDSSMOC that were observed at least twice. The symbols with error bars connected by the solid line show the distribution of the *a* colour change for a subset of 2289 asteroids brighter than $r = 19$ and with the difference in angles from the opposition smaller than 1.5°. Its equivalent Gaussian width, determined from the interquartile range, is 0.053 mag. The dash-dotted line shows the distribution of the *a* colour change between two epochs for 21 000 stars brighter than $r = 19$. Its width, which indicates the measurement error for *a* colour, is 0.023 mag. This figure is available in colour in the on-line version of the journal on *Synergy*.

from 'red' asteroids using the $i - z$ colour (J02). The *a* and $i - z$ colours are strongly correlated with dynamical family membership (Ivezić et al. 2002c, hereafter I02c). Hereafter, we chose the *a* colour as the primary quantity to study asteroid colour variability.

3.1 Detection of asteroid colour variability in SDSSMOC

The observed distribution of the *a* colour change between two epochs, Δa, for 2289 selected asteroids, is shown by symbols (with error bars) in Fig. 1. Its equivalent Gaussian width determined from the interquartile range (hereafter 'width') is 0.053 mag. The expected width based on the formal errors reported by the SDSS photometric pipeline ('photo', Lupton et al. 2001) is 0.02 mag, indicating that the observed Δa distribution reflects intrinsic asteroid colour changes. However, the formal errors may not be correct. In order to determine the measurement accuracy for the *a* colour, we use 21 000 stars with $r < 19$ that were observed twice. The dashed line in Fig. 1 shows their Δa distribution. Its width is 0.023 mag, in agreement with the expectations based on formal errors.

Subtracting the error distribution width of 0.023 mag in quadrature, the intrinsic *a* colour rms variation is 0.04 mag. While Fig. 1 demonstrates that this measurement is statistically highly significant, in the remainder of this section we test for the presence of spurious observational effects that could be responsible for the observed asteroid colour variation.

3.2 Tests for spurious observational effects

3.2.1 Colour change versus asteroid velocity

Although the formal photometric errors for stars are correct, asteroids move during observations and their motion could in principle affect the photometric accuracy. While this effect should be negligible (the images are not strongly trailed), we test for it by correlating

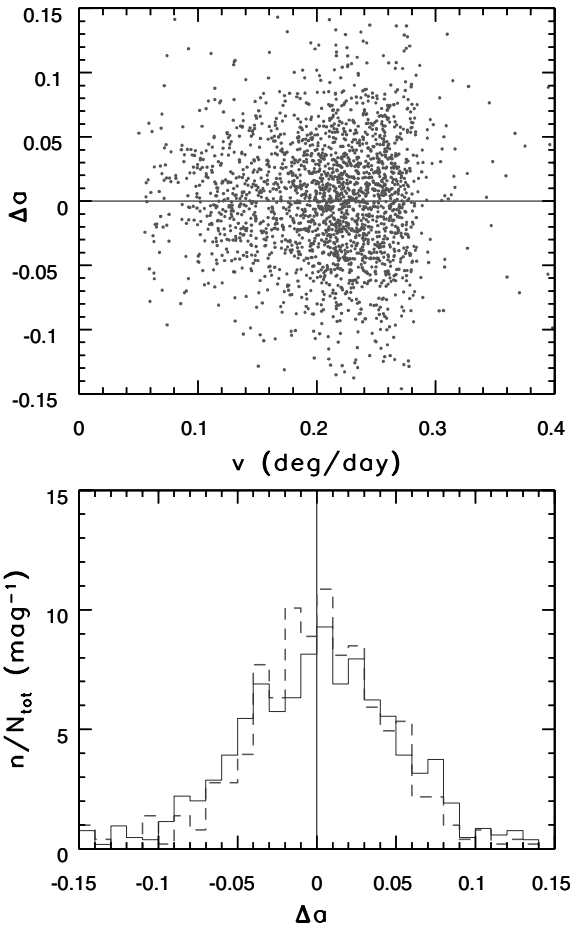

Figure 2. The upper panel shows the *a* colour change between two epochs for the same asteroids as in Fig. 1, as a function of the object's velocity. The bottom panel compares the width of the distribution of the *a* colour change for 511 objects with $0.10 < v < 0.18$ (dashed line) and for 1065 objects with $v > 0.22$ deg d^{-1} (solid line). Note that the two histograms are statistically indistinguishable, indicating that the colour measurement is not affected by the object's apparent velocity. This figure is available in colour in the on-line version of the journal on *Synergy*.

Δa with the object's velocity. If the photometric accuracy is lower for moving objects, the Δa distribution width should increase with magnitude of the object's velocity. The Δa versus v diagram is shown in the top panel in Fig. 2. The bottom panel compares the width of the Δa distribution for two subsamples selected by velocity. The dashed line shows the Δa distribution for 511 objects with 0.1 deg d^{-1} $< v <$ 0.18 deg d^{-1}, and the solid line for 1065 objects with $v > 0.22$ deg d^{-1}. As evident, the two histograms are statistically indistinguishable.

3.2.2 Colour change versus apparent brightness

The photometric errors typically increase with apparent magnitude of the measured object. While the adopted faint limit ($r < 19$) is sufficiently bright that SDSS photometric errors are nearly independent of magnitude (Ivezić et al. 2002c), we test this expectation by correlating Δa with the mean apparent magnitude in Fig. 3. The bottom panel compares the width of the Δa distribution for two subsamples selected by $r < 17$ (dashed line, 214 objects) and by $18.5 < r < 19$ (solid line, 898 objects). There is no significant difference between the two histograms. Relaxing the magnitude

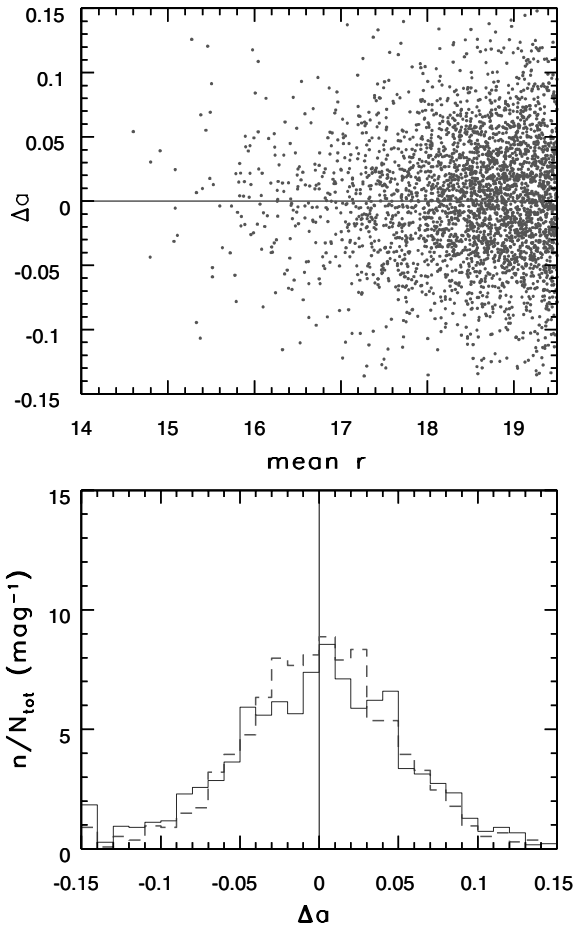

Figure 3. The upper panel shows the a colour change between two epochs for the same asteroids as in Fig. 1, as a function of the object's apparent magnitude. The bottom panel compares the width of the distribution of the a colour change for 214 objects with $r < 17$ (dashed line) and for 898 objects with $18.5 < r < 19$ (solid line). Note that the two histograms are statistically indistinguishable, indicating that the colour measurement is not affected by the object's apparent magnitude. This figure is available in colour in the on-line version of the journal on *Synergy*.

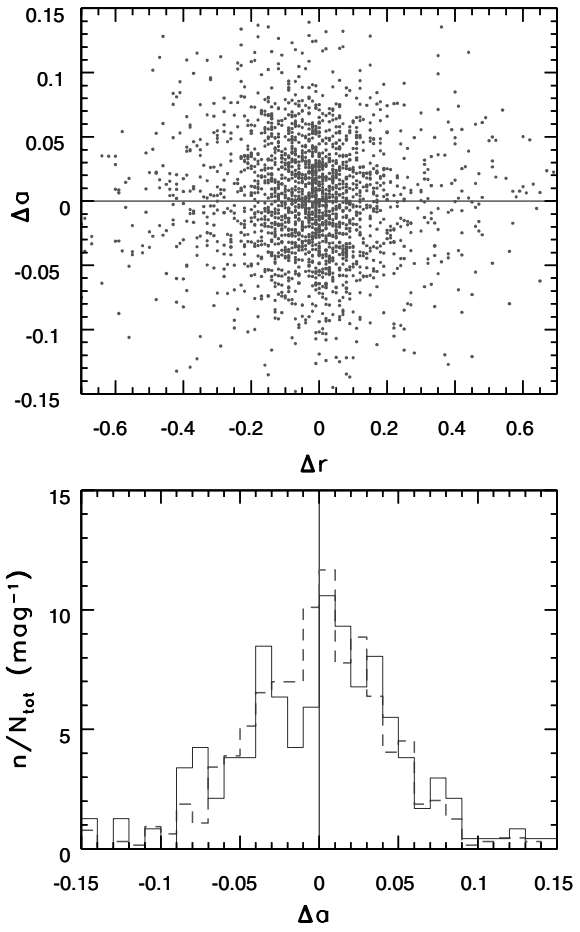

Figure 4. The upper panel shows the a colour change between two epochs for the same asteroids as in Fig. 1, as a function of the change in the r band apparent magnitude The bottom panel compares the width of the distribution of the a colour change for 645 objects with $|\Delta(r)| < 0.05$ (dashed line) and for 1644 objects with $|\Delta(r)| > 0.05$ (solid line). Note that the two histograms are statistically indistinguishable, indicating that the colour measurement is not correlated with the change of the object's apparent magnitude. This figure is available in colour in the on-line version of the journal on *Synergy*.

cut to $r < 20$ yields the same null result with a sample size increased by a factor of 2. We have also tested the Δa versus Δr dependence, illustrated in Fig. 4, and did not detect any correlation.

3.2.3 Colour change versus angle from the opposition

In order to minimize the opposition effect (see section 6.1 in I01), the maximum change of the angle from the opposition (between two observations) in the analysed sample is constrained to 1.5° (this limit may be slightly too conservative, since we find no correlation between Δa and the *change* of the angle from the opposition for changes as large as 10°). To exclude the possibility that the colour change is affected by the *mean* angle from the opposition, we analyse Δa as a function of this angle in Fig. 5. There is no discernible correlation.

Unlike the colour change, which is not correlated with the angle from the opposition, the change of magnitudes between two epochs is strongly correlated with this angle, as expected. The top panel in Fig. 6 shows the dependence of Δr on the change of the angle from the opposition. The comparison of Δr distributions for two ranges of the angle change (0°–1° as the solid line and 2°–10° as the dashed line) are shown in the bottom panel. As evident, even when asteroids are observed at practically the same position, Δr has a wide distribution, mostly due to asteroid rotation. We find that the Δr distribution can be well fitted by a sum of two Gaussians with widths of 0.08 mag and 0.35 mag and amplitude ratio 2:1, shown as the dash-dotted line. The measured Δr distribution can be used to constrain the distributions of asteroid axes ratios and rotational periods. Such an analysis, while interesting in its own right, is beyond the scope of this paper.

3.2.4 Effects of non-simultaneous measurements

The SDSS photometric measurements are obtained in the order r–i–u–z–g, and the elapsed time between the first (r) and last (g) measurement is ∼5 min. The asteroid brightness variation during this time, even if achromatic, introduces a bias in the colour measurement. For example, if an asteroid is observed during the rising part of its light curve, the $r - i$ colour is biased red, and the $g - r$ colour is biased blue. Also, due to fixed filter order, the colour biases should

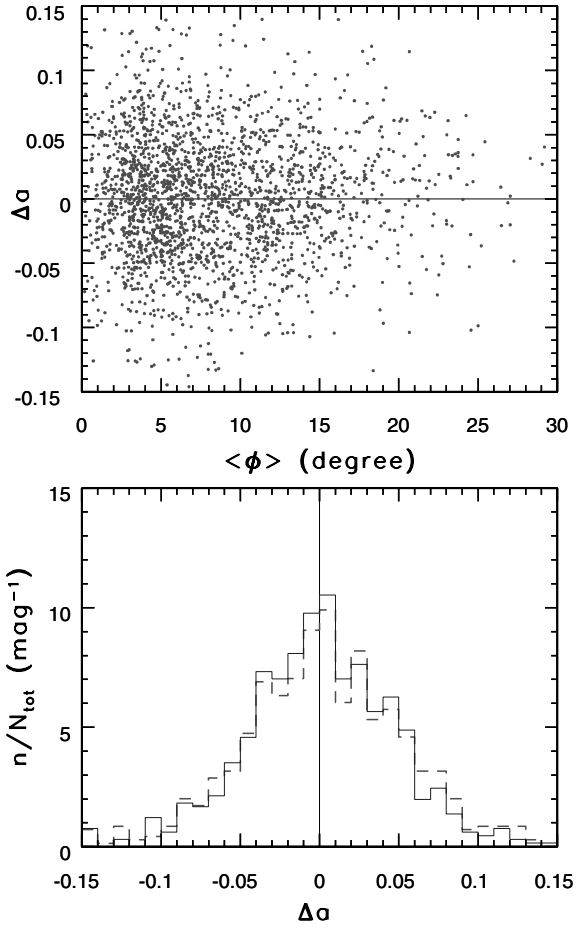

Figure 5. The upper panel shows the a colour change between two epochs for the same asteroids as in Fig. 1, as a function of the mean angle from the opposition. The bottom panel compares the width of the distribution of the a colour change for 712 objects with $\phi < 5^\circ$ (dashed line) and for 664 objects with $10^\circ < \phi < 20^\circ$ (solid line). Note that the two histograms are statistically indistinguishable, indicating that the colour measurement is not correlated with the mean angle from the opposition. This figure is available in colour in the on-line version of the journal on *Synergy*.

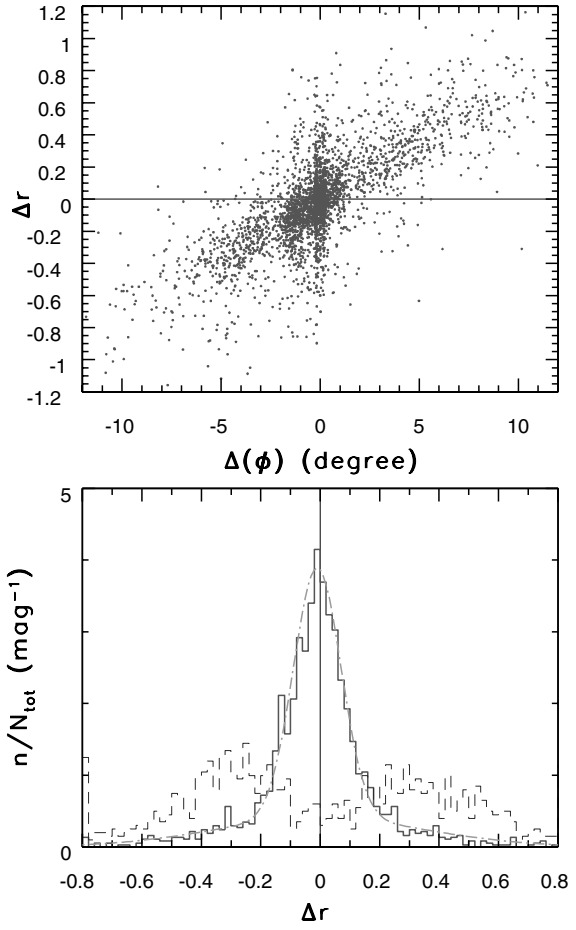

Figure 6. The upper panel shows the change of r magnitude for the full sample, as a function of the change of the angle from the opposition. The bottom panel compares the Δr distributions for two ranges of the angle change: 0°–1° as the solid line and 2°–10° as the dashed line. The former is well fitted by a sum of two Gaussians (see text) shown as the dash-dotted line. This figure is available in colour in the on-line version of the journal on *Synergy*.

be correlated. The expected correlations are

$$\Delta(g-r)/\Delta(u-g) \sim -2, \quad \Delta(r-i)/\Delta(g-r) \sim -0.25,$$
$$\Delta(i-z)/\Delta(r-i) \sim 2, \quad \Delta(g-r)/\Delta(i-z) \sim -2,$$
$$\Delta(r-i)/\Delta(u-g) \sim 0.5, \quad \Delta(i-z)/\Delta(u-g) \sim 1.$$

With the conservative assumptions that the typical rotational period is as short as 2 h, and that the peak-to-peak amplitude is as large as 0.5 mag, the expected rms contribution is the largest for $g-r$ colour and equal to ∼0.03 mag, while for $r-i$ colour it is less than 0.01 mag.

Fig. 7 shows the six possible correlations of the four SDSS colours. The rms scatter of each colour is also displayed in the figure. As evident, the variations in all four colours are too large by a factor of a few to be explained by any plausible rotation parameters. Furthermore, the slopes of the expected correlations, shown by the dashed lines, are not supported by the data. We conclude that the non-simultaneous nature of SDSS colour measurements is not significantly contributing to the observed colour variation.

The $u-g$ and $i-z$ colour changes show the largest width. We have verified that imposing a magnitude cut (<19) on the u and z magnitudes does not decrease the scatter, i.e. the large widths are not caused by the lower sensitivity of these two bands.

3.2.5 Correlated colour variations

Fig. 7 demonstrates that some colour pairs [e.g. $\Delta(r-i)$ versus $\Delta(g-r)$] show correlations with a slope that cannot be explained by the examined instrumental effects. We characterize the observed correlations by their linear regression, the rms of the fit and the linear correlation coefficient C. All the fits cross the origin (the zeroth-order coefficients do not differ significantly from 0). We determined the following correlations:

$$\Delta(g-r) = -0.13(1)\Delta(u-g), \quad \text{rms} = 0.06, \quad C = -0.26; \quad (2)$$

$$\Delta(r-i) = -0.40(2)\Delta(g-r), \quad \text{rms} = 0.06, \quad C = -0.42; \quad (3)$$

$$\Delta(i-z) = -0.51(2)\Delta(r-i), \quad \text{rms} = 0.07, \quad C = -0.42; \quad (4)$$

$$\Delta(i-z) = -0.13(2)\Delta(g-r), \quad \text{rms} = 0.07, \quad C = -0.12. \quad (5)$$

There are some noteworthy aspects of this test. First, the change of $u-g$ colour does not correlate with the change of $r-i$ and $i-z$ colours, although the scatter of $\Delta(u-g)$ is much higher than for the other colours. Also, the colour indices $u-X$, where $X =$

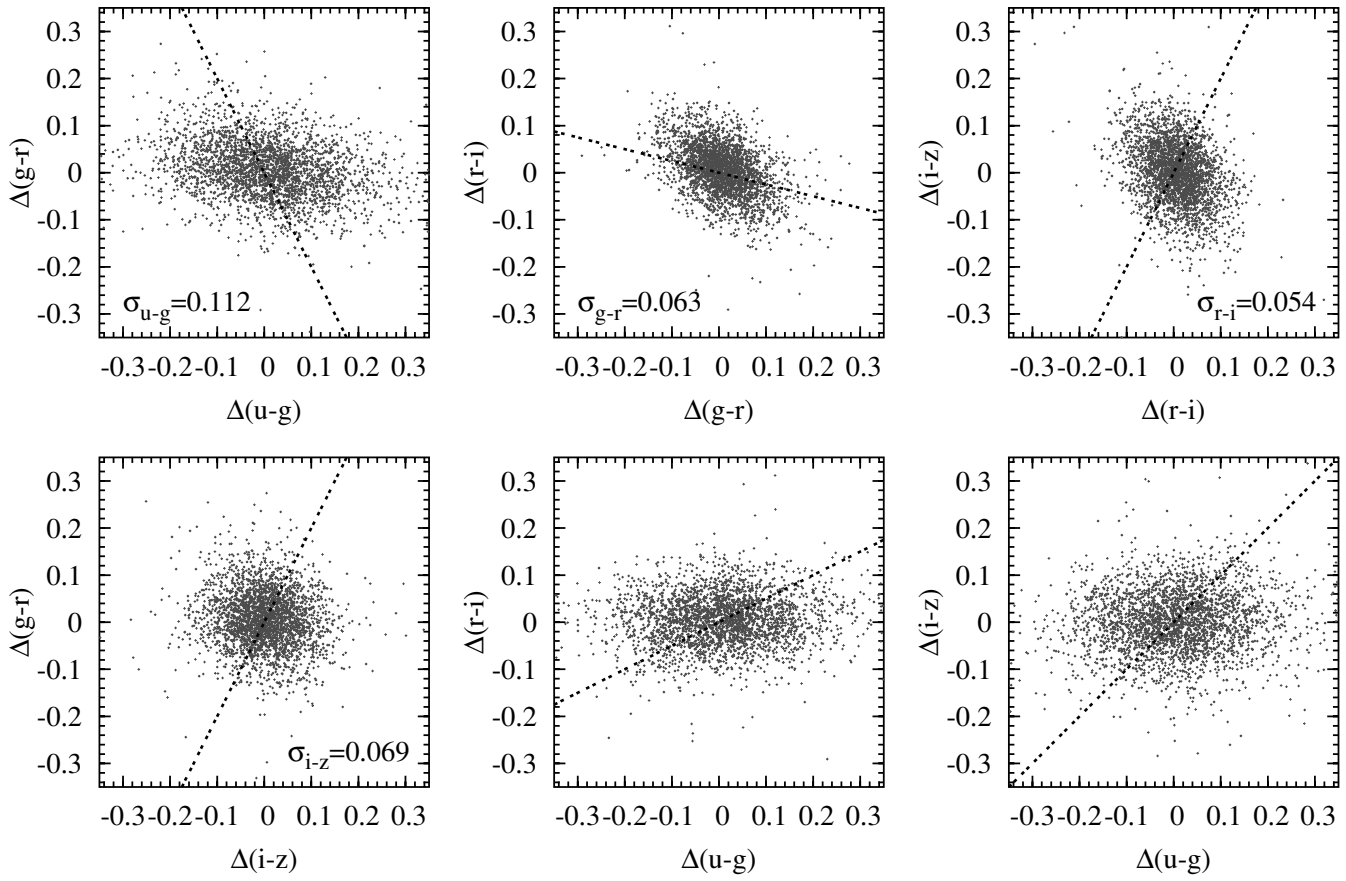

Figure 7. Correlations between the changes of four SDSS colours for the same asteroids as in Fig. 1. The dashed lines show the expected slopes if non-simultaneous observations and fast, large-amplitude variability produce significant bias in colour measurements (see Section 3.2.4). This bias is not supported by the displayed data. This figure is available in colour in the on-line version of the journal on *Synergy*.

g, r, i, z, do not correlate with any other colour index that does not include X. This is consistent with a hypothesis that the blue part of the spectrum is affected by a process that causes no colour variation of the red colours.

3.2.6 Variability-induced motion in colour–colour diagrams

The changes of $r - i$ and $g - r$ colours, which are used to define colour a, seem to be weakly correlated, with the median slope $\Delta(r - i) \sim -0.4\ \Delta(g - r)$ given by (3). This implies that, on average, the line connecting two observations in this diagram is more aligned with the second principal axis, which is perpendicular to a, than with the a-axis. Using the definition of the second principal colour, hereafter named p,

$$p \equiv 0.45(g - r) - 0.89(r - i) - 0.11, \quad (6)$$

we constructed the principal colour diagram shown in the top panel in Fig. 8. Note that this diagram is simply a rotated version of the $r - i$ versus $g - r$ diagram. In this panel we simply plot the mean value of each principal colour, while in the middle panel we connect two individual measurements by lines, for a small subset of objects with $18 < r < 18.3$ (to avoid crowding) and a change in each colour of at least 0.03 mag. As evident, for objects with large colour variations, the changes of the two principal colours seem to be somewhat correlated, with slope larger than unity. That is, the p colour varies more than the a colour. In the bottom panel we show the change of p colour versus the change of a colour for all the objects in the 'high-quality' subsample, as well as the rms scatter in each colour.

The observed variability of the p colour appears nearly sufficient to explain its single-measurement distribution width of $\sim$0.05 mag (the rms width of the change in that colour is 1.33 of its single-epoch width, i.e. only slightly smaller than the expected value of 1.41 if the variability was the only reason for its finite value). In order to test this hypothesis, we use a subsample of 541 asteroids that were observed at least four times. The distribution width for the mean p colour, obtained by averaging the four measurements, is expected to be smaller than that measured for any individual epoch. On the other hand, no significant difference in the distribution widths is expected for the a colour. The distributions shown in Fig. 9 suggest that the variability contributes significantly to the p colour distribution width, and much less to the width of each individual mode in the a colour distribution.

Since the variability-induced motion in the p versus a colour–colour diagram is more aligned with the p-axis than with the a-axis, over 90 per cent of asteroids have the same a-based classification (<0 versus >0) in different epochs. The same behaviour also indicates that the colour variability cannot be explained as due to mixing of two basic materials, corresponding to C and S types, on the asteroid surfaces. We will return to this point in Section 5.

3.3 Repeatability of colour variations

The suite of tests in this section suggest that the observed colour variations are not an artefact (either observational or caused by phenomena such as differential opposition effect). However, the lack of any correlation with physical parameters, such as colour,

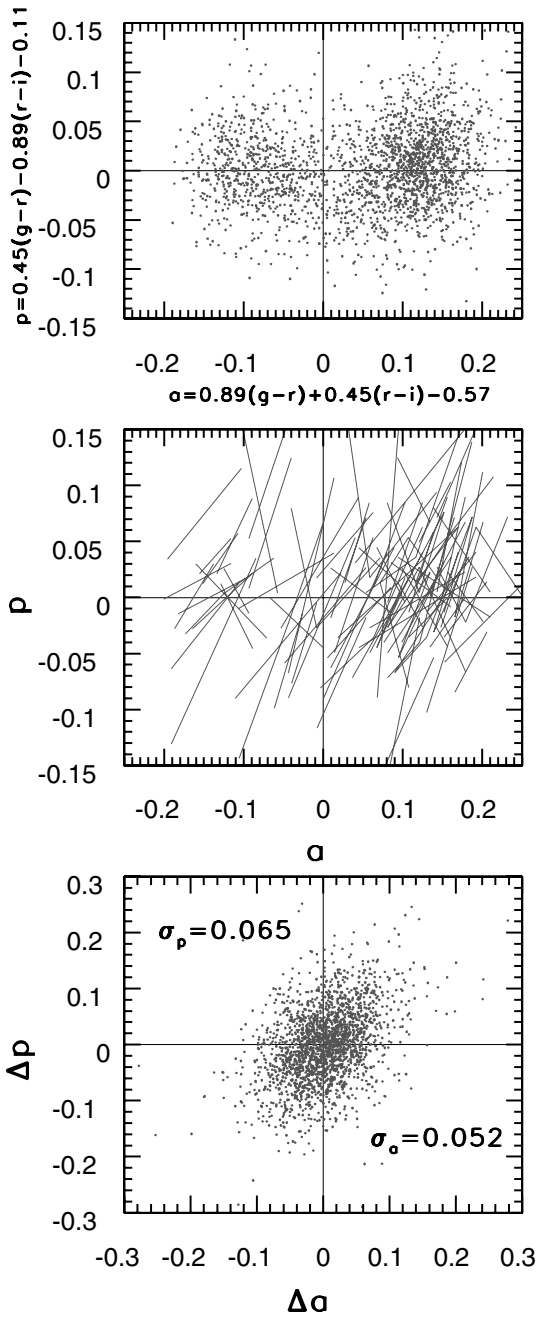

Figure 8. The top panel shows the asteroid principal colour diagram, constructed with the mean colours for two measurements. In the middle panel two individual measurements are connected by lines, for a small subset of objects with $18 < r < 18.3$ and a change in each colour of at least 0.03 mag. Note that for objects with large colour variations, the changes of the two principal colours seem to be somewhat correlated. The bottom panel shows the change of p colour versus the change of a colour for all the objects in the 'high-quality' subsample, as well as the rms scatter in each colour. This figure is available in colour in the on-line version of the journal on *Synergy*.

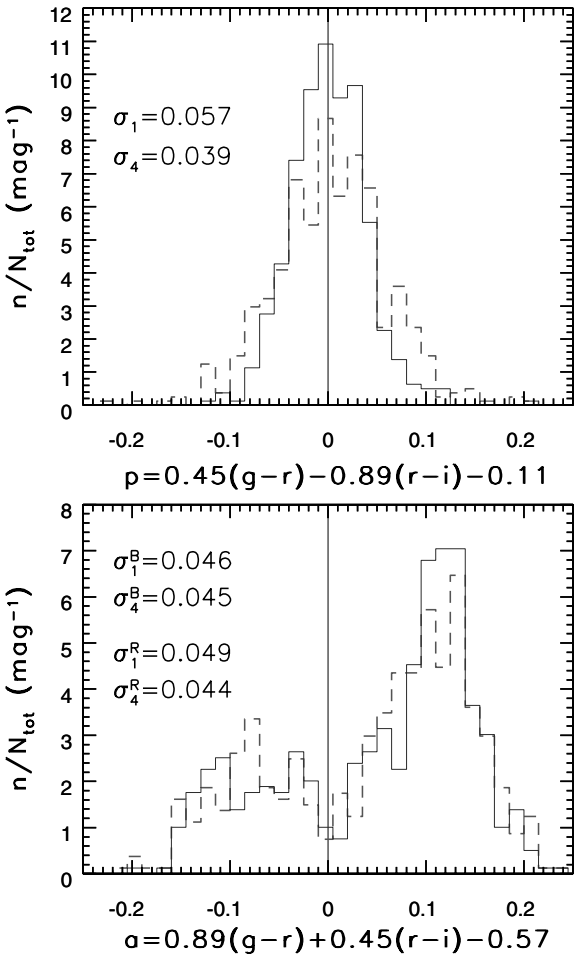

Figure 9. The comparison of the p (top panel) and a (bottom panel) colour distributions obtained by averaging four measurements (solid lines) for 541 asteroids, and those for individual measurements (dashed lines). The σ values are the distribution widths, subscripted 1 for single epoch and 4 for average measurements. The widths for the a colour distribution are determined separately for objects with $a < 0$ (superscript B) and $a > 0$ (superscript R). Note that the width of the p colour distribution is 1.46 larger for single epoch measurements, while the a colour distribution does not change appreciably. This figure is available in colour in the on-line version of the journal on *Synergy*.

size and family membership, discussed in the next section, may be elegantly explained as being caused by some 'hidden' random error contribution, for example a problem introduced by the processing software. Here we present a test which demonstrates that at least in one aspect the observed colour variation is not random.

If it is true that asteroids exhibit a varying degree of colour variability, as they do, for example, for single-band variability, then the colour changes detected in two independent pairs of observations may correlate to some degree. At the same time, such a correlation would give credence to the reliability of the measurements. We use a subsample of 541 asteroids that were observed at least four times to test whether such a correlation exists. The top panel in Fig. 10 plots the change of a colour in a pair of observations versus the change in another independent pair of observations. We have verified that the marginal distributions in each coordinate are indistinguishable.

To illustrate this point, in the bottom panel we compare the distributions of the a colour change in one pair of observations for two subsamples selected by the a colour change in the other independent pair of observations, as marked by the dashed lines in the top panel. If the colour changes in the two pairs of observations are uncorrelated, then the two histograms should be indistinguishable. However, they are clearly different, indicating that these independent observations 'know' about each other!

In order to quantify the statistical significance of the difference between the two histograms, we perform two tests. A two-sample

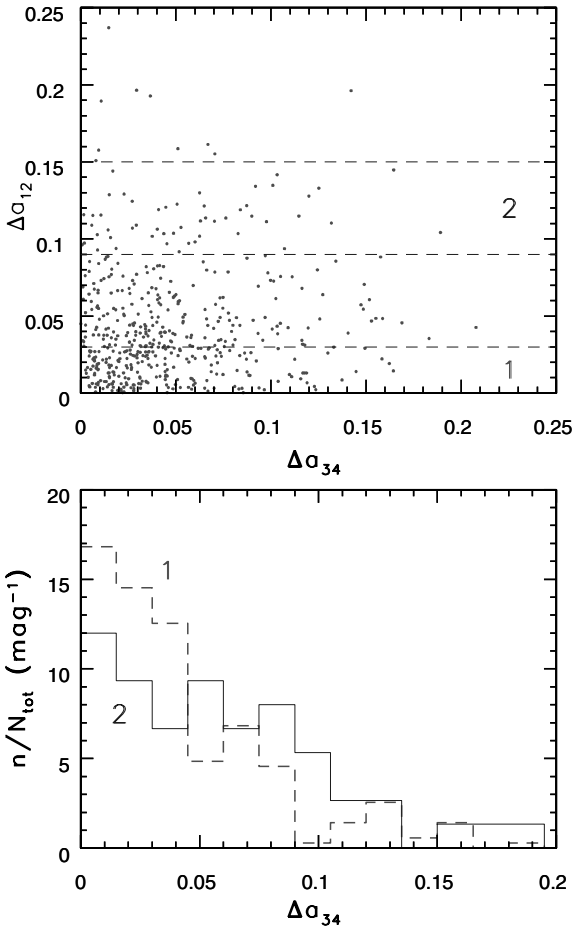

Figure 10. The top panel plots the changes of *a* colour in two independent pairs of observations (change in the first pair versus the change in the second pair) for 541 asteroids observed at least four times. The bottom panel compares the histograms of *a* colour change in one of the two pairs of observations, for two subsets selected by the *a* colour change in the other pair of observations, as marked by the dashed lines in the top panel (see text). Note that the two distributions are different, indicating that these independent observations 'know' about each other. The same conclusion is obtained when the axes are reversed. This figure is available in colour in the on-line version of the journal on *Synergy*.

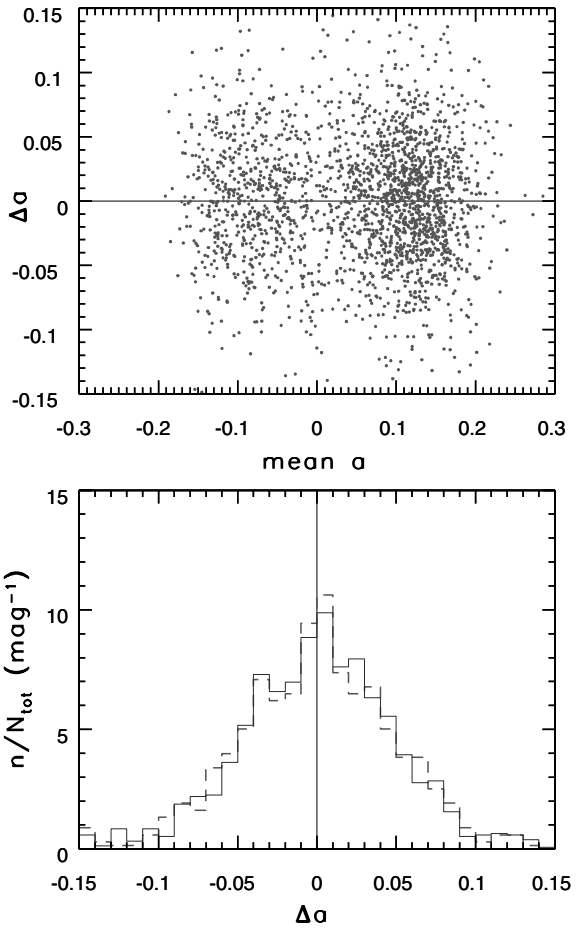

Figure 11. The upper panel shows the *a* colour change between two epochs for the same asteroids as in Fig. 1, as a function of the mean *a* colour. The bottom panel compares the distributions of the *a* colour change for 689 objects with mean $a < 0$ and 1585 objects with mean $a > 0$. Note that the two histograms are statistically indistinguishable, indicating that the colour measurement is not correlated with the asteroid's *a* colour (which is a good proxy for taxonomic classification). This figure is available in colour in the on-line version of the journal on *Synergy*.

Kolmogorov–Smirnov test (Lupton 1993) indicates that the histograms are different at a confidence level of more than 99 per cent. Another test, proposed by Efron & Petrosian (1992), which uses the entire 2D sample, indicates that the two variables are correlated at a confidence level of 95 per cent. The somewhat lower confidence level than for the first test is probably due to the contribution of points with small colour changes, whose distribution may be randomized by photometric errors.

We conclude that objects with large colour variations in one pair of observations tend to show relatively large colour variations in the other, independent, pair of observations. This difference strongly suggests that the observed colour variations are real, and also indicates that colour variations are stronger for some asteroids than for others.

4 APPARENTLY RANDOM NATURE OF COLOUR VARIABILITY

The series of tests discussed in the preceding section demonstrate that the detection of asteroid colour variability is robust. In this section we attempt to find correlations between colour variability and other parameters such as colours (a good proxy for taxonomic classes), absolute magnitude (i.e. size) and family membership.

4.1 Colour variability as a function of mean colours

The position of an asteroid in the principal colour diagram (the top panel in Fig. 8) is a good proxy for its taxonomic classification (I01). Thus, a dependence of colour variability on taxonomic type would show up as a correlation between the change of *a* colour and its mean value. We show the scatter plot of these two quantities in the upper panel in Fig. 11. The bottom panel compares the distributions of the *a* colour change for 689 objects with mean $a < 0$ (dominated by the C-type objects) and 1585 objects with mean $a > 0$ (dominated by the S-type objects). The two histograms are statistically indistinguishable.

While the mean-colour-selected objects (blue versus red) appear to show the same *a* colour change distributions, it may be possible that the objects with the largest Δr or Δa would show different principal colour distributions. We repeat the asteroid principal colour diagram constructed with the mean colours (already shown

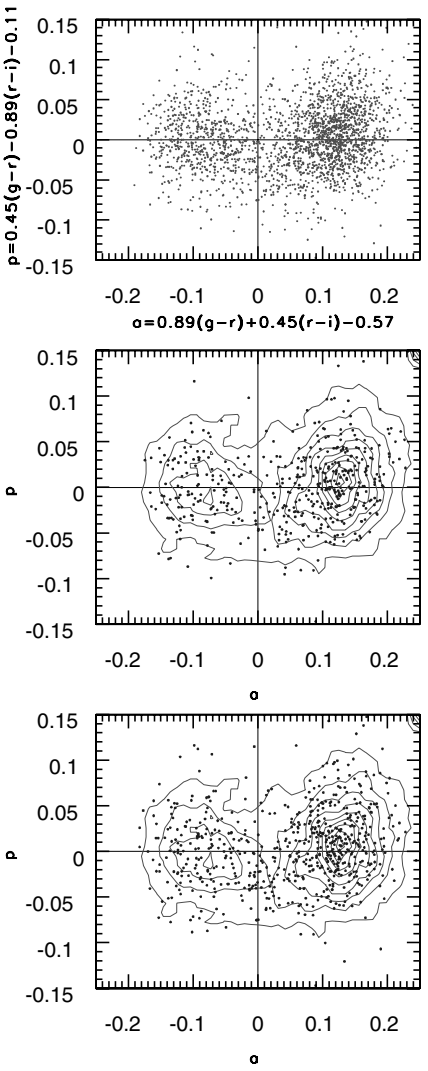

Figure 12. The top panel shows the asteroid principal colour diagram, constructed with the mean colours for two measurements, for the whole sample. The same distribution is shown by linearly spaced isodensity contours in the middle and bottom panels. The dots in the middle panel represent objects with a change in the r magnitude of at least 0.2 mag. The dots in the bottom panel represent objects with a change in the a colour of at least 0.05 mag. Note that objects with large changes of magnitudes and colours appear to show the same mean principal colour distribution as the full sample. This figure is available in colour in the on-line version of the journal on *Synergy*.

in Fig. 8) in the top panel in Fig. 12. The same distribution is shown by linearly spaced isodensity contours in the middle and bottom panels. The dots in the middle panel represent objects with a change in the r magnitude of at least 0.2 mag. The dots in the bottom panel represent objects with a change in the a colour of at least 0.05 mag. There is no discernible difference between the colour distributions for the whole sample and that for the highly variable objects.

4.2 Colour variability as a function of absolute magnitude

Asteroids of different size may exhibit different colour variability. The closest proxy for size, in the absence of direct albedo measurements, is absolute magnitude. Fig. 13 shows a correlation between Δa and the absolute magnitude H. The displayed range of H roughly corresponds to the 1–10 km size range. The bottom panel compares the width of the Δa distribution for 97 objects with $10 < H < 13$ (dashed line) and for 505 objects with $15 < H < 16$ (solid line). The two histograms are statistically indistinguishable, indicating that the colour change is not correlated with the asteroid's absolute magnitude (i.e. size). However, we emphasize that the dynamic range of probed sizes is fairly small.

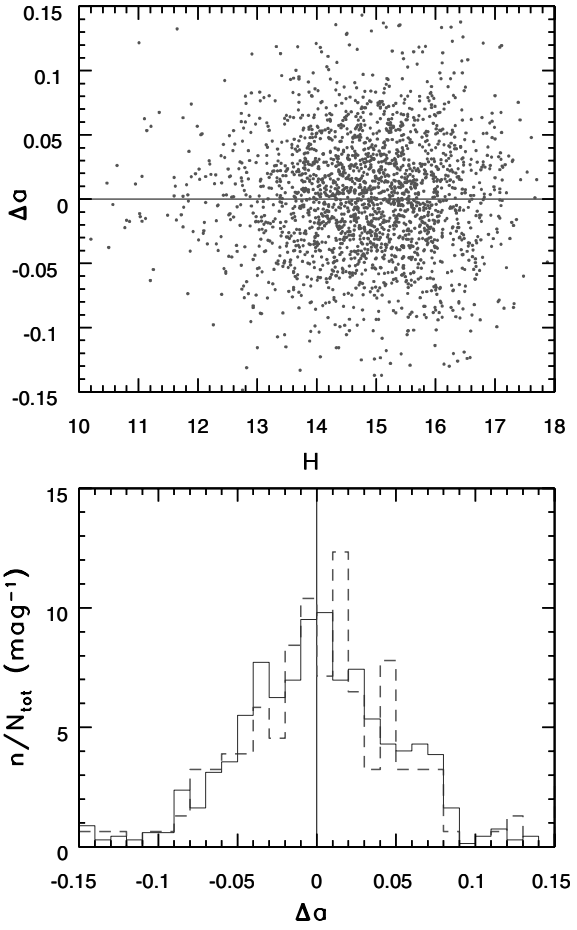

Figure 13. The upper panel shows the a colour change between two epochs for the same asteroids as in Fig. 1, as a function of the absolute magnitude. The bottom panel compares the width of the distribution of the a colour change for 97 objects with $10 < H < 13$ (dashed line) and for 505 objects with $15 < H < 16$ (solid line). Note that the two histograms are statistically indistinguishable, indicating that the colour measurement is not correlated with the asteroid's absolute magnitude (i.e. size, in the approximate range 1–10 km). This figure is available in colour in the on-line version of the journal on *Synergy*.

4.3 Colour variability as a function of family membership

SDSS colours are a good proxy for taxonomic classification, and can be efficiently used to recognize at least three colour groups (J02).

Table 1. The definitions of asteroid families in a_p – sin i – e space.

Groups	a_p	sin i	e
Flora	2.16–2.32	0.04–0.125	0.105–0.18
Vesta	2.28–2.41	0.10–0.135	0.07–0.125
Nysa-Polana	2.305–2.48	0.03–0.06	0.13–0.21
Eunomia-Adeona	2.52–2.72	0.19–0.26	0.12–0.19
Eos	2.95–3.10	0.15–0.20	0.04–0.11
Themis	3.03–3.23	0–0.6	0.11–0.20

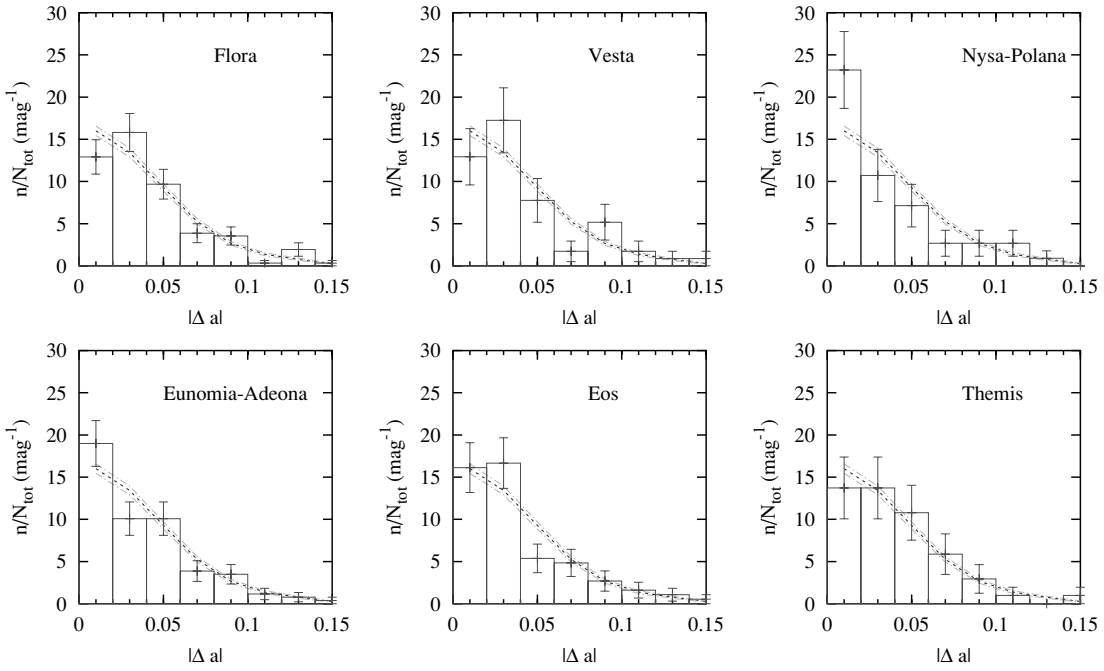

Figure 14. The distribution of $|\Delta a|$ for individual asteroid families (boxes with error bars) is compared to the distribution for the whole sample, shown by lines (mean $\pm\sigma$). The families are defined by regions in the space spanned by proper orbital elements (see Table 1 and text). This figure is available in colour in the on-line version of the journal on *Synergy*.

I02c showed by correlating asteroid dynamical families and SDSS colours that indeed there are more than just three 'shades': many families have distinctive and uniform colours. Motivated by their finding, we obtain a more detailed classification of asteroids using dynamical clustering and correlate it with variability properties.

We define families by three-dimensional boxes in the space spanned by proper orbital elements (the boundaries are summarized in Table 1), using the results from Zappala et al. (1995). There are six families with more than 50 members in the sample analysed here. The comparison of $|\Delta a|$ and $|\Delta r|$ distributions for individual families with those for the whole sample are shown in Figs 14 and 15, respectively. In order to assess quantitatively whether there is any family that differs in its variability properties from the rest of the sample, we performed two-sample Kolmogorov–Smirnov tests. None of the families listed in Table 1 was found to differ from the mean values for the whole sample at a confidence level greater than

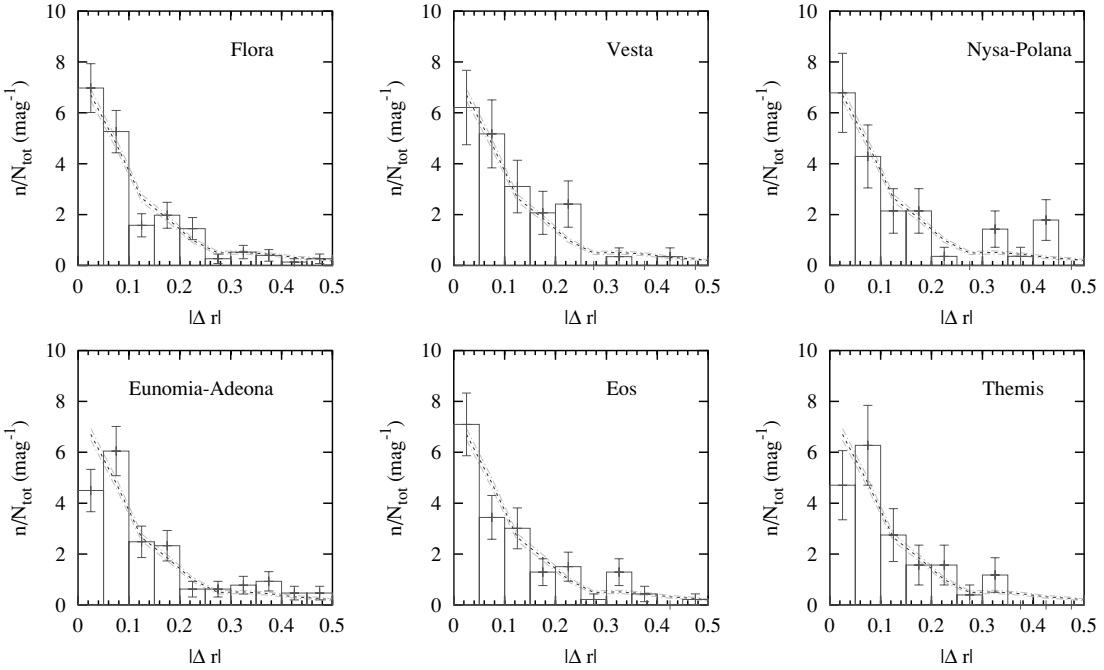

Figure 15. Same as Fig. 14, except that the absolute value of the *r*-band brightness variation is shown. This figure is available in colour in the on-line version of the journal on *Synergy*.

95 per cent. We conclude that all the examined families show similar variability properties.

5 DISCUSSION AND CONCLUSIONS

The detection of colour variability for the large sample of asteroids discussed here represents a significant new constraint on the physical properties and evolution of these bodies. The random nature of this variability, implied by the lack of apparent correlations with asteroid properties such as mean colours, absolute magnitude and family membership, could be interpreted as due to some hidden random photometric error. However, several lines of evidence argue that this explanation is unlikely. First, the magnitude of the observed effect (0.06–0.11 mag) is so large that such photometric errors would have to be noticed in numerous other studies and tests based on SDSS photometric data. If such an error only shows up for moving objects, then the colour variability should increase with the apparent velocity, an effect that is not observed (see Fig. 2). Secondly, independent pairs of observations, discussed in Section 3.4, seem to 'know' about each other: objects with large colour variation in one pair of observations tend to show relatively large colour variation in another pair of observations. This fact cannot be explained by random photometric errors. Thirdly, the colour variation is not entirely random in the principal colours diagram, as discussed in Section 3.3. There is a preferred direction for variability-induced motion in this diagram, and the scatter in principal colours is significantly different ($\sigma_p \sim 1.33\sigma_a$). Were the colour variability to be caused by random photometric errors, it would not be correlated with the distribution of asteroid principal colours.

The observed colour variability implies inhomogeneous albedo distribution over an asteroid surface. Although the colour variability is fairly small, it suggests that large patches with different colour than their surroundings exist on a significant fraction of asteroids. For example, consider a limiting case of an asteroid with two different hemispheres, one with C-type material, and one with S-type material. In this case the peak-to-peak amplitude of its *a* colour variability would be only 0.2 mag, with rms $\sim$ 0.05 mag,[3] even under the most favourable condition of the rotational axis perpendicular to the line of sight. Taking into account a distribution of the angle between the rotational axis and the line of sight would decrease these values further. Without detailed modelling it is hard to place a lower limit on the fraction of surface with complementary colour to explain the observed colour variations. However, using simple toy models and colours typical for C- and S-type asteroids, we find that this fraction must be well over 10 per cent. The features seen in spatially resolved colour images of Eros obtained by the *NEAR* spacecraft (Murchie et al. 2002) support such a conclusion.

A simple explanation for the existence of patches differing in colour from their surroundings is the deposition of material (e.g. silicates on C-type asteroids and carbonaceous material on S-type asteroids) by asteroid collisions. However, such surfaces would exhibit colour variations preferentially aligned with the *a* colour axis, contrary to the observations. For a given fraction of asteroid surface affected by the deposition of new material, the large difference in albedos of silicate and carbonaceous surfaces would probably produce different amplitudes of colour variability for S- and C-type asteroids (due to a large difference in their albedos), a behaviour that is not supported by the data. Thus, the colour variability cannot be explained as due to patches of S-like and C-like material scattered across an asteroid surface.

A plausible cause for optically inhomogeneous surface is space weathering. This phenomenon includes the effects of bombardment by micrometeoroids, cosmic rays, solar wind and ultraviolet radiation, and may alter the chemistry of the surface material (Zeller & Rouce 1967). Recent spacecraft data indicate that these processes may be very effective in the reddening and darkening of asteroid surfaces (Chapman 1996). In this interpretation the $u - g$ colour should show the largest variation (Hendrix & Vilas 2003), and this is indeed supported by the data presented here (see Fig. 7). It is not clear, however, how such processes could result in fairly large isolated surface inhomogeneities.

An interesting explanation for surface inhomogeneities is the effects of cratering. Using *NEAR* spacecraft measurements, Clark et al. (2001) find 30–40 per cent albedo variations on the Psyche crater wall on Eros. Such a large effect could perhaps produce colour variations consistent with observations. However, it seems premature to draw conclusions without detailed modelling.

Irrespective of the mechanism(s) responsible for the observed colour variations, our results indicate that this is a rather common phenomenon. We conclude by pointing out that the sample presented here will be enlarged by a factor of a few in a year or two because SDSS is still collecting data, and the size of the known object catalogue, needed to link the observations, is also growing. Furthermore, the faint limit of the known object catalogue is also improving, and will result in a larger size range probed by the sample. Apart from SDSSMOC, the upcoming (in 5–10 yr) deep synoptic surveys such as *Pan-STARRs* and *LSST* will produce samples of size and quality that will dwarf the sample discussed here, and provide additional clues about the causes of asteroid colour variability.

[3] The colour light curve would be biased red because of the factor of 4 difference in the visual albedos.

ACKNOWLEDGMENTS

This work has been supported by the Hungarian OTKA Grants T034615, FKFP Grant 0010/2001, Szeged Observatory Foundation and Pro Renovanda Cultura Hungariae Foundation DT 2002/maj.21. I acknowledges generous support by Princeton University.

Funding for the creation and distribution of the SDSS Archive has been provided by the Alfred P. Sloan Foundation, the Participating Institutions, the National Aeronautics and Space Administration, the National Science Foundation, the US Department of Energy, the Japanese Monbuhagakusho, and the Max Planck Society. The SDSS website is www.sdss.org. The Participating Institutions are the University of Chicago, Fermilab, the Institute for Advanced Study, the Japan Participation Group, the Johns Hopkins University, the Max-Planck-Institute for Astronomy (MPIA), the Max-Planck-Institute for Astrophysics (MPA), New Mexico State University, Princeton University, the United States Naval Observatory, and the University of Washington.

REFERENCES

Azabajian K. et al., 2003, AJ, 126, 2081
Baliunas S., Donahue R., Rampino M. R., Gaffey M. J., Shelton J. C., Mohanti S., 2003, Icarus, 163, 35
Binzel R. P., Gaffey M. J., Thomas P. C., Zellner B. H., Storrs A. D., Wells E. N., 1997, Icarus, 128, 95
Blanco C., Catalano S., 1979, Icarus, 40, 359
Bowell E., 2001, Introduction to ASTORB. Available from ftp://ftp.lowell.edu/pub/elgb/astorb.html
Bowell E., Lumme K., 1979, in Gehrels T., ed., Asteroids. Univ. Arizona Press, Tucson, p. 132
Chapman C. R., 1996, Meteoritics, 31, 699

Clark B. E. et al., 2001, Meteoritics Planet. Sci., 36, 1617
Degewij J., Tedesco E. F., Zellner B. H., 1979, Icarus, 40, 364
Efron B., Petrosian V., 1992, ApJ, 399, 345
Fukugita M., Ichikawa T., Gunn J. E., Doi M., Shimasabu K., Schneider D. P., 1996, AJ, 111, 1748
Gammelgaard P., Kristansen L. K., 1991, A&A, 244, 544
Hendrix A. R., Vilas F., 2003, 34th Annual Lunar and Planetary Science Conf., March 17–21. League City, Texas
Ivezić Ž. et al., 2001, AJ, 122, 2749 (I01)
Ivezić Ž., Jurić M., Lupton R. H., Tabachnik S., Quinn T., 2002a, in Tyson J. A., Wolff S., eds, Proc. SPIE 4836, Survey and Other Telescope Technologies and Discoveries. Int. Soc. Opt. Eng., Bellingham, WA, p. 98
Ivezić Ž. et al., 2002b, AJ, 124, 2943
Ivezić Ž. et al., 2002c, astro-ph/0301400 (I02c)
Jurić M. et al., 2002, AJ, 124, 1776 (J02)
Lupton R. H., 1993, Statistics in Theory and Practice. Princeton Univ. Press, Princeton, NJ
Lupton R. H., Gunn J. E., Ivezić Ž., Knapp G. R., Kent S., Yasuda N., 2001, in Harnden F. R., Jr, Primini F. A., Payne H. E., eds, ASP Conf. Ser. Vol. 238, Astronomical Data Analysis Software and Systems X. Astron. Soc. Pac., San Francisco, p. 269
Magnusson M., 1991, A&A, 243, 512
Metcalf J. H., 1907, ApJ, 25, 264
Milani A., 1999, Icarus, 137, 269
Mottola S., Gonano-Beurer M., Green S. F., McBride N., Brinjes J. C., di Martino M., 1994, Planet. Space Sci., 42, 21
Murchie S. et al., 2002, Icarus, 155, 145
Pravec P., Harris A. W., 2000, Icarus, 148, 12
Russell H. N., 1906, ApJ, 24, 1
Schober H. J., Schroll A., 1982, Sun and Planetary System. Reidel, Dordrecht, p. 258
Sekiguchi T., Boehnhardt H., Hainaut O. R., Delahodde C. E., 2002, A&A, 385, 281
Sheppard S. S., Jewitt D. C., 2002, AJ, 124, 1775
Shoemaker E., Williams J. G., Helin E. F., Wolfe R. F., 1979, in Gehrels T., ed., Asteroids. Univ. Arizona Press, Tucson, p. 253
Szabó Gy. M., Csák B., Sárneczky K., Kiss L. L., 2001, A&A, 375, 285
Wisniewski W. Z., 1976, Icarus, 28, 87
Wisniewski W. Z., Michałowski T. M., Harris A. W., McMillan R. S., 1997, Icarus, 126, 395
Zappala V., Bemdjoya Ph., Cellino A., Farinella P., Froeschlé C., 1995, Icarus, 116, 291
Zeller E. J., Rouce L. B., 1967, Icarus, 7, 372
Zellner B., 1979, in Gehrels T., ed., Asteroids. Univ. Arizona Press, Tucson, p. 783
Zellner B., Tholen D. J., Tedesco E. F., 1985, Icarus, 61, 355
Zellner B. H., Albrecht R., Binzel R. P., Gaffey M. J., Thomas P. C., Storrs A. D., Wells E. N., 1997, Icarus, 128, 83

This paper has been typeset from a TEX/LATEX file prepared by the author.